Circular Photoinduced Electron Transfer in a Donor-Acceptor-Acceptor Triad

Christopher B. Larsen*[a] and Oliver S. Wenger*[a]

Abstract: Herein is communicated an electron donor-acceptor-acceptor (D-A_1-A_2) triad that provides the first proof-of-concept for a photoinitiated molecular circuit. Upon photoexcitation into an optical charge-transfer transition between D and A_1, subsequent thermal electron-transfer from A_1^- to A_2 is followed by geometric rearrangement in the D^+-A_1-A_2^- charge-separated state to form an ion-pair contact. This facilitates 'forward' charge-recombination between A_2^- and D^+ that completes the molecular circuit, with an estimated quantum efficiency of 4% in toluene at 298 K.

The concepts of fully-integrated molecular circuitry and single-molecule circuitry have long been considered the ultimate goal in the field of molecular electronics.[1] Despite significant attention having been paid to molecules that act as individual circuitry components, such as wires, switches and rectifiers,[2] there have been to date no reports of single molecules that can act as a molecular circuit.

Photoinduced electron transfer (ET) across donor-bridge-acceptor (D-B-A) compounds in solution has been widely investigated as a proxy for one-dimensional molecular wires and to gain deeper insight into ET mechanisms.[3] Often, the goal was to achieve long-lived electron-hole pairs for temporary energy storage, and to decelerate thermal charge recombination (CR) events as much as possible.[4] Common strategies to achieve this include the use of rigid rod-like backbones that help maximizing the donor-acceptor distance and the use of multiple donors or acceptors that permit establishment of a redox gradient.[5]

Our approach is conceptually different since we aimed at circular electron transfer rather than long-lived electron-hole pairs. With this specific goal in mind, we synthesized and explored a molecular (D-A_1-A_2) triad, comprised of a triarylamine (TAA) donor (D), a primary benzothiadiazole (BTD) acceptor (A_1), and a secondary anthraquinone (AQ) acceptor (A_2), linked together by thiophene (th) bridges (Scheme 1). The **TAA-th-BTD-th-AQ** compound can conformationally rearrange in the charge-separated (CS) state to form an ion-pair contact between $TAA^{\bullet+}$ ($D^{\bullet+}$) and $AQ^{\bullet-}$ ($A_2^{\bullet-}$), creating a pseudo-macrocyclic structure that facilitates a pathway for forward (circuit-like) CR, such that three sequential unidirectional ET steps can occur within the circuit (left part of **Scheme 1**). While there have been prior studies of electron delocalization in conjugated macrocycles and 'nanorings',[6] to our knowledge there exists currently no method to control the directionality of the movement of the charge in them, and thus our D-A_1-A_2 triad provides an important proof-of-concept. The formation of the ion-pair contact in the CS state is facilitated by the *ortho* substitution pattern around the central BTD acceptor (A_1) and the conformational flexibility of the bridging th groups, allowing the Coulombic attraction between $TAA^{\bullet+}$ ($D^{\bullet+}$) and $AQ^{\bullet-}$ ($A_2^{\bullet-}$) to bring them into close proximity.

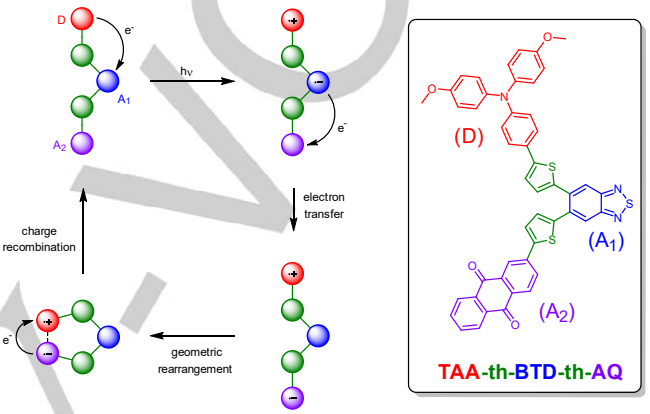

Scheme 1. Proposed mechanism for the charge-transfer processes in the target D-A_1-A_2 triad. The overall result is circular photoinduced electron transfer. Red = TAA, blue = BTD, purple = AQ, green = th.

Synthesis and characterisation data are presented in the supporting information (SI) on pages S2-S6.

Electronic absorption and photoluminescence spectra of **TAA-th-BTD-th-AQ** and two control compounds, **TAA-th-BTD** and **TAA-th-BTD-th-TAA** (see Figure S1 for their complete molecular structures), recorded in CH_2Cl_2 are presented in Figure 1. **TAA-th-BTD**, in which the TAA donor and BTD acceptor are free to adopt a coplanar arrangement, exhibits an intense low energy TAA→BTD CT band at 447 nm (black trace, ε = 22,300 M^{-1} cm^{-1}), consistent with previously reported D-A systems.[7] The second lowest band (351 nm, ε = 25,800 M^{-1} cm^{-1}) appears consistent with a th→BTD CT transition. In the symmetrical **TAA-th-BTD-th-TAA** reference compound, the *ortho* substitution pattern around the central BTD acceptor sterically inhibits adoption of a coplanar arrangement, and consequently the TAA→BTD CT band is hypsochromically shifted to ca. 415 nm (green trace) such that it becomes merely visible as a shoulder to the higher energy th→BTD CT band (355 nm).

The key compound **TAA-th-BTD-th-AQ** (blue trace in Figure 1) has the lowest energy optical transition occur at essentially the same energy and intensity as for **TAA-th-BTD-th-TAA**, implying that the lowest energy transition is still TAA→BTD CT in nature (solid blue arrow no. 1 in Figure 1). Whilst the higher energy transitions present in **TAA-th-BTD-th-TAA** also appear to be retained in **TAA-th-BTD-th-AQ**, it is evident that there are also new transitions. Specifically, we note the presence of a low energy shoulder on the 349 nm band that we assign to th→AQ

[a] Dr. C. B. Larsen, Prof. Dr. O. S. Wenger
Department of Chemistry
University of Basel
St Johanns-Ring 19, CH-4056 Basel, Switzerland
E-mail: christopherbryan.larsen@unibas.ch
oliver.wenger@unibas.ch

Supporting information for this article is given via a link at the end of the document.

CT (solid blue arrow no. 2) based on electrochemical data (Table S1), as well as TD-DFT calculations (Table S6).

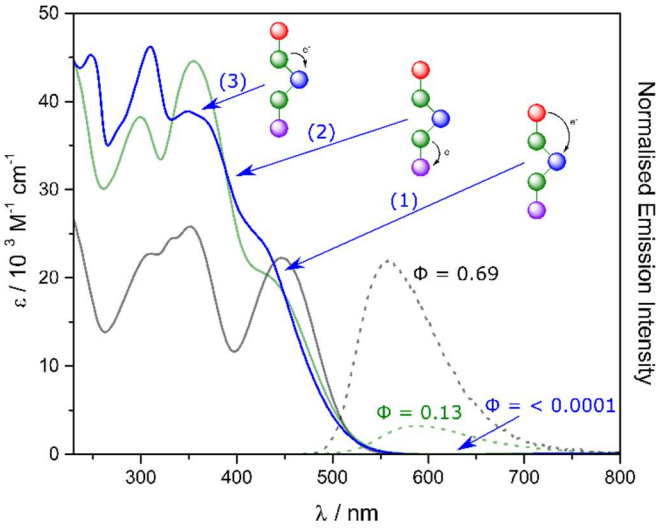

Figure 1. Electronic absorption (solid lines, recorded in CH_2Cl_2) and photoluminescence spectra (dashed lines, λ_{ex} = 450 nm, recorded in toluene) of **TAA-th-BTD** (black), **TAA-th-BTD-th-TAA** (green) and **TAA-th-BTD-th-AQ** (blue). Schematics depict the nature of optical transitions for **TAA-th-BTD-th-AQ**.

The control compounds, **TAA-th-BTD** and **TAA-th-BTD-th-TAA**, both exhibit ^{1}CT emission (black and green dotted traces in Figure 1), with λ_{em} of 557 nm (ϕ_{PL} = 0.69, τ = 4.0 ns) and 585 nm (ϕ_{PL} = 0.13, τ = 1.7 ns), respectively, in toluene (see SI pages S15-S16 for details). The shift to longer wavelengths is consistent with the narrowing electrochemical gap between the TAA oxidation and BTD reduction going from **TAA-th-BTD** to **TAA-th-BTD-th-TAA** (Table S1), and is therefore assigned as ^{1}**TAA$^{\bullet+}$-th-BTD$^{\bullet-}$-th-TAA** in nature.

The **TAA-th-BTD-th-AQ** key compound exhibits only extremely weak emission at 585 nm (φ_{PL} < 0.0001). As the magnitude in shift of λ_{em} from that of **TAA-th-BTD** is the same as for **TAA-th-BTD-th-TAA** ($\Delta\lambda_{em} \approx$ 28 nm, ~0.1 eV), as is the magnitude of narrowing electrochemical gap between the TAA oxidation and BTD reduction relative to **TAA-th-BTD** ($\Delta\Delta G_{ET}^0$ = 0.09 eV, Table S1), this emission is characterised as ^{1}**TAA$^{\bullet+}$-th-BTD$^{\bullet-}$-th-AQ** in nature. The extremely low φ_{PL} is consistent with quenching of the **TAA$^{\bullet+}$-th-BTD$^{\bullet-}$-th-AQ** excited state by rapid intramolecular ET to the ^{1}**TAA$^{\bullet+}$-th-BTD-th-AQ$^{\bullet-}$** CS state (i. e. further ET from the primary (A_1) to the secondary acceptor (A_2)), as demonstrated in the following.

Spectroelectrochemical data (recorded in CH_2Cl_2) and UV-Vis transient absorption (TA) spectra (recorded in toluene) of **TAA-th-BTD-th-AQ** are presented and compared in Figure 2. The TA difference spectrum (black trace in Figure 2c) exhibits bleaching below 450 nm, as well as broad absorption features at 540 and in the 650-800 nm range, consistent with the spectroelectrochemical signatures obtained for AQ$^{\bullet-}$ (blue trace in Figure 2b) and TAA$^{\bullet+}$ (red trace in Figure 2a). The combined data in Figure 2 clearly indicate the formation of the **TAA$^{\bullet+}$-th-BTD-th-AQ$^{\bullet-}$** ($D^{\bullet+}$-A_1-$A_2^{\bullet-}$) CS state. The TA signal (Figure 2c) forms within the time resolution of the pump laser (~10 ns).

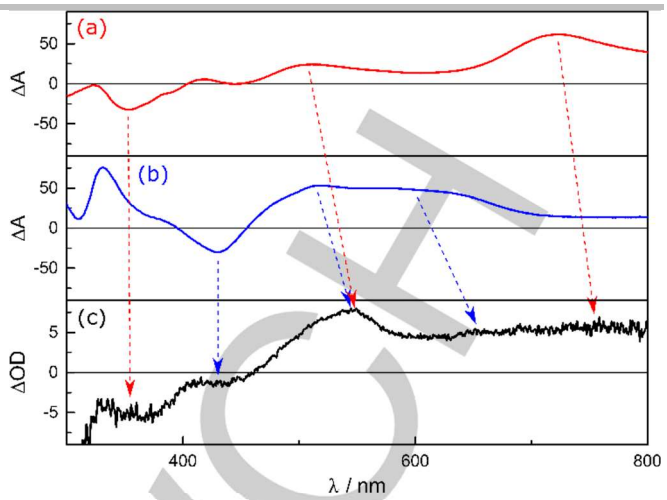

Figure 2. ΔA spectra obtained upon electrochemical (a) TAA oxidation (red trace) and (b) AQ reduction (blue trace) of **TAA-th-BTD-th-AQ**, recorded in CH_2Cl_2 in presence of 0.1 M Bu_4NPF_6, with applied potentials of 0.9 and -1.1 V vs SCE, respectively, and (c) the transient absorption ΔOD spectrum of **TAA-th-BTD-th-AQ** recorded in toluene at 298 K (black trace, λ_{ex} = 410 nm) immediately following excitation and time-integrated over 200 ns.

Decay of the TA signal at 540 nm in de-aerated toluene at 298 K is biexponential, with lifetimes (τ) of 12.1 (60%) and 31.9 (40%) µs (Table 1, Figure S11). The lifetimes of these states are quenched upon introduction of $^3O_2$, indicating that they are triplet in nature. As the rate of intersystem crossing (ISC) in organic molecules is slow compared to the rate of fluorescence, ET from BTD$^{\bullet-}$ to AQ likely occurs within the singlet manifold. As back-ET from AQ$^{\bullet-}$ to BTD is energetically disfavoured by 0.5 eV (Table S1), this state is thermodynamically trapped and slow ISC into the triplet manifold can occur. Alternatively, some reports have demonstrated that in strongly-coupled systems, direct electron-transfer from a singlet state to a triplet can occur through spin-orbit coupling induced ET.[8] Given that th bridges typically imbue strong electronic coupling, this represents a viable alternative mechanism for the formation of the ^{3}**TAA$^{\bullet+}$-th-BTD-th-AQ$^{\bullet-}$** CS state.

Table 1. Lifetimes from decay of the transient absorption signal at 540 nm, recorded as de-aerated 30 µM solutions at 298 K (λ_{ex} = 410 nm).

Solvent	τ_1 / µs	τ_2 / µs
Toluene	12.1 (60%)	31.9 (40%)
1,4-Dioxane	8.31 (22%)	53.9 (78%)
THF	7.76 (17%)	40.0 (83%)

A molar extinction coefficient for the oxidised TAA of 17100 M^{-1} cm^{-1} at 720 nm in CH_2Cl_2 was obtained from chemical oxidation experiments (Figure S9). Assuming minimal contribution from reduced AQ at this wavelength, a quantum yield for the population of the ^{3}**TAA$^{\bullet+}$-th-BTD-th-AQ$^{\bullet-}$** ($D^{\bullet+}$-A_1-$A_2^{\bullet-}$) CS state can be estimated as 0.07 (SI, page S16) in toluene at 298 K. A Jablonski diagram depicting the excited-state decay channels that lead to this low quantum yield is presented in Figure S14.

Upon changing solvent to 1,4-dioxane or THF, the signal decays become triexponential and do not return completely to baseline

(Figure S11, left), consistent with the introduction of intermolecular quenching mechanisms.[9] The lifetimes of the two shorter-lived components (τ_1 and τ_2) are comparable to those in toluene, but the relative contribution of τ_1 decreases and that of τ_2 increases (Table 1). In principle, the two decay times τ_1 and τ_2 could reflect different ground-state conformers that undergo CR with different kinetics. In order to clarify this point, TA measurements in a frozen 2-methyltetrahydrofuran (MeTHF) matrix at 77 K were insightful. The resulting TA decays are monoexponential (with a lifetime of 1.68 ms; Figure S11, right), and since multiple different (frozen) ground-state conformers must be present under these conditions, it seems highly unlikely that different ground-state conformers would be responsible for the multiexponential decay behaviour observed in fluid solution at 298 K. This strongly suggests that τ_1 and τ_2 are related to different ^{3}**TAA$^{\bullet+}$-th-BTD-th-AQ$^{\bullet-}$** CS state conformers dominated by significantly different CR mechanisms. We hypothesised that conformational rearrangement in the CS state could lead to the formation of an ion-pair contact between between TAA$^{\bullet+}$ and AQ$^{\bullet-}$, facilitating through ion-pair CR[10] akin to the previously reported 'harpooning' mechanism.[11] Such ion-pairs exist in an equilibrium between a closed and open form, and as back-ET from AQ$^{\bullet-}$ to BDT is energetically disfavoured by 0.5 eV (Table S1), the most likely mechanisms are tunnelling from AQ$^{\bullet-}$ to TAA$^{\bullet+}$ through the covalent backbone of the triad (through-bond pathway), predominantly in the open form, and a through ion-pair pathway, predominantly in the closed form.

As direct experimental evidence for such a conformational change is very difficult to obtain, we turned first to TD-DFT calculations and then to temperature-dependent transient absorption studies (*vide infra*). B3LYP TD-DFT calculations predict the formation of a hydrogen-bond between a TAA$^{\bullet+}$ proton and an AQ$^{\bullet-}$ oxygen in both the S_1 and T_1 excited states, which correspond to the **TAA$^{\bullet+}$-th-BTD-th-AQ$^{\bullet-}$** CS state (Figure 3b), not present in the S_0 (ground) state (Figure 3a, Table S8). The calculated energy difference between the HOMO (TAA-based) and LUMO (AQ-based) models the difference in redox potentials of the TAA and AQ within 10% error (Table S4), validating the calculation.

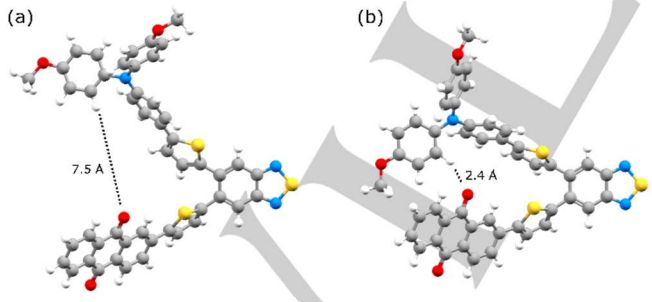

Figure 3. Geometry-optimised structures of **TAA-th-BTD-th-AQ** in (a) the ground state (S_0) and; (b) the lowest energy triplet excited state (T_1), corresponding to the **TAA$^{\bullet+}$-th-BTD-th-AQ$^{\bullet-}$** ($D^{\bullet+}$-A_1-$A_2^{\bullet-}$) CS state, optimised at the B3LYP 6-31G(d,p) level of theory with a toluene SCRF solvent field.

As the solvent polarity is increased, the electron-hole pair in the CS state can be stabilised to a greater degree, shifting the equilibrium to a more open conformation (away from the ion-paired conformation). As such, the contribution of the ion-paired conformer to the excited-state decay should decrease with respect to that of the open form. The trends in τ_1 and τ_2 (Table 1) therefore suggest that τ_1 is related to the ion-paired conformer (decreasing from 60% to 22% and 17% between toluene, dioxane and THF) and τ_2 to the open conformer. Furthermore, due to the rigidity of the frozen matrix,[12] the ground-state geometry (Figure 3a) is locked in, preventing conformational rearrangement and formation of an ion-pair contact in the frozen glass. The monoexponential decay at 77 K is therefore consistent with through-bond CR. Due to large equilibrium torsion angles around the central BTD unit and long through-bond donor-acceptor distance in the CS state (Table S9), the long lifetime of τ_2 is consistent with a through-bond mechanism.[9] However, it is not possible to relate the solution decay times τ_1 and τ_2 directly to CR rate constants of individual conformers, because the rate of interchange between open and closed conformations affects the observable time constants. In fact, the latter are expected to be a complicated combination of the various rate constants (see SI page S23).[13] Therefore, the observed rate constants for the decay of the two conformers, k_{obs-1} (τ_1^{-1}) and k_{obs-2} (τ_2^{-1}), do not directly represent specific CR mechanisms.

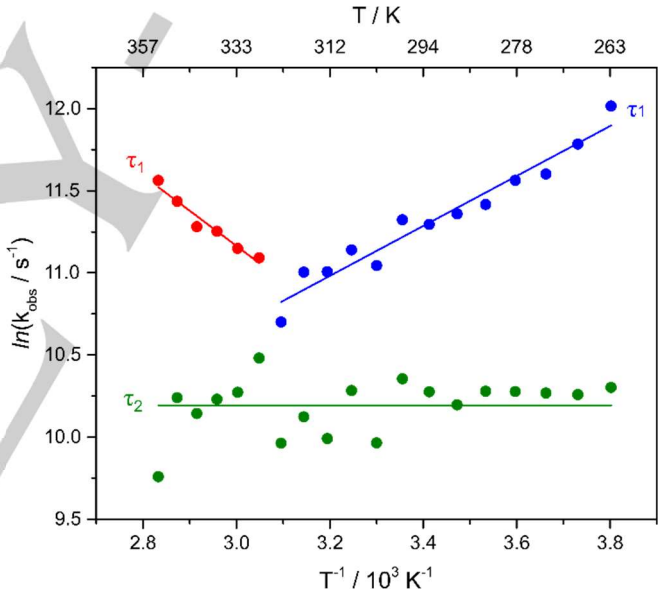

Figure 4. Arrhenius plots for **TAA-th-BTD-th-AQ** in toluene for τ_1 (red and blue) and τ_2 (green).

Nevertheless, variable temperature TA lifetime measurements in toluene (Figure 4) support our interpretation that τ_1 is dominated by a through ion-pair CR pathway in the closed conformer. The temperature dependence of τ_1 clearly exhibits two temperature regimes: a low temperature regime in which k_{obs-1} decreases with increasing temperature (blue circles), and a high temperature regime in which k_{obs-1} increases with increasing temperature (red circles). The lower temperature regime, which yields an apparent negative activation energy, is consistent with behaviour previously reported for intermolecular charge-transfer complexes.[14] For example, Fukuzumi *et al.* demonstrated for hydride-transfer reactions that an apparent negative activation energy is only possible through the formation of a charge-transfer complex as a reaction intermediate.[14a] This is consistent with our

hypothesis that τ_1 is primarily related to the closed conformer and that the dominant CR pathway in this conformer is across the $TAA^{\bullet+}$ / $AQ^{\bullet-}$ ion-pair contact. In this regime, increasing temperature shifts the equilibrium to a more open conformation (away from the ion-paired conformation), decreasing k_{obs-1} and leading to the apparent negative activation energy. k_{obs-2} exhibits no observable temperature-dependence (green circles), and this is not unprecedented for through-bond CR.[9] Between 290 and 340 K, the relative contribution of τ_1 decreases with respect to τ_2 (Figure S13), further consistent with thermal disruption of the ion-paired conformation. In the higher temperature regime, the relative contributions of τ_1 and τ_2 appear to plateau, and τ_1 reflects ordinary behaviour with a positive activation energy (red circles in Figure 4). This is suggestive that increased thermal molecular motion leads to a greater number of spontaneous 'encounter complex' ion-paired conformers, in which CR occurs predominantly through the ion-pair contact or potentially through solvent-space.[15]

Thus, the combination of solvent- and temperature-dependent transient absorption studies with DFT calculations clearly points towards direct (forward) electron transfer from $AQ^{\bullet-}$ to $TAA^{\bullet+}$ across a short ion-pair contact, made possible as a result of the conformational flexibility of our D-A_1-A_2 triad. This process is in competition with ordinary through-bond CR as commonly observed in more rigid rod-like donor-bridge-acceptor constructs. Given an estimated quantum yield of 0.07 for formation of the **$TAA^{\bullet+}$-th-BTD-th-$AQ^{\bullet-}$** CS state in toluene at 298 K (SI, page S20), and a 60% contribution of CR from the ion-paired conformer at that temperature in toluene (Table 1, top left entry), a quantum efficiency for electrons travelling in a complete circuit can be estimated at 0.04 under these conditions.

In conclusion, we have herein communicated a donor-acceptor-acceptor triad that provides the first proof-of-concept for a photoinitiated single-molecule circuit. The key design principles that have permitted such behaviour are: (i) excitation into an optical charge-transfer band to afford directly a primary charge-separated state ($D^{\bullet+}$-$A_1^{\bullet-}$-A_2) with high efficiency (Scheme 1, top right corner); (ii) rapid subsequent onward electron transfer to yield a very long-lived secondary charge-separated state ($D^{\bullet+}$-A_1-$A_2^{\bullet-}$) (Scheme 1, bottom right); (iii) geometric reorganisation in this charge-separated state to form an ion-pair contact between $A_2^{\bullet-}$ and $D^{\bullet+}$ (Scheme 1, bottom left).

We envisage that upon optimisation of the quantum efficiency of the photoinitiated molecular circuit, such systems may be expanded beyond a simple 'three-station' circuit to much more complex systems able to perform specific electronic functions and become incorporated as electronic devices. Furthermore, the controllable circular flow of electrons may have an associated magnetic field, enabling the development of a fundamentally new class of (photoswitchable) molecular magnets.

Acknowledgements

C. B. L. acknowledges a Swiss Government Excellence Postdoctoral Scholarship for Foreign Scholars. Financial support by the Swiss National Science Foundation through grant number 200021_146231/1 is gratefully acknowledged. The authors thank Dr. M. Kuss-Petermann and Dr. X. Guo for insightful discussion, and Dr. D. Häussinger for NMR support.

Keywords: electron transfer • donor-acceptor systems • time-resolved spectroscopy • charge transfer • ion pairs

[1] a) M. Kiguchi, *Single-molecule Electronics*, Springer, **2016**; b) E. Scheer, *Molecular electronics: an introduction to theory and experiment, Vol. 1*, World Scientific, **2010**; c) F. Fassioli, D. G. Oblinsky, G. D. Scholes, *Faraday Discuss.* **2013**, *163*, 341-351.

[2] a) J. R. Heath, M. A. Ratner, *Phys. Today* **2003**, *56*, 43-49; b) L. Sun, Y. A. Diaz-Fernandez, T. A. Gschneidtner, F. Westerlund, S. Lara-Avila, K. Moth-Poulsen, *Chem. Soc. Rev.* **2014**, *43*, 7378-7411; c) C. J. Lambert, *Chem. Soc. Rev.* **2015**, *44*, 875-888.

[3] a) M. Cordes, A. Kottgen, C. Jasper, O. Jacques, H. Boudebous, B. Giese, *Angew. Chem. Int. Ed.* **2008**, *47*, 3461-3463; b) V. A. Montes, C. Perez-Bolivar, N. Agarwal, J. Shinar, P. Anzenbacher, *J. Am. Chem. Soc.* **2006**, *128*, 12436-12438; c) M. T. Indelli, C. Chiorboli, L. Flamigni, L. De Cola, F. Scandola, *Inorg. Chem.* **2007**, *46*, 5630-5641; d) P. P. Edwards, H. B. Gray, M. T. J. Lodge, R. J. P. Williams, *Angew. Chem. Int. Ed.* **2008**, *47*, 6758-6765; e) V. Lloveras, J. Vidal-Gancedo, T. M. Figueira-Duarte, J. F. Nierengarten, J. J. Novoa, F. Mota, N. Ventosa, C. Rovira, J. Veciana, *J. Am. Chem. Soc.* **2011**, *133*, 5818-5833; f) A. C. Benniston, A. Harriman, *Chem. Soc. Rev.* **2006**, *35*, 169-179; g) C. Lambert, C. Risko, V. Coropceanu, J. Schelter, S. Amthor, N. E. Gruhn, J. C. Durivage, J. L. Brédas, *J. Am. Chem. Soc.* **2005**, *127*, 8508-8516; h) P. J. Low, *Dalton Trans.* **2005**, 2821-2824; i) U. Pfaff, A. Hildebrandt, D. Schaarschmidt, T. Ruffer, P. J. Low, H. Lang, *Organometallics* **2013**, *32*, 6106-6117; j) D. C. O'Hanlon, B. W. Cohen, D. B. Moravec, R. F. Dallinger, M. D. Hopkins, *J. Am. Chem. Soc.* **2014**, *136*, 3127-3136; k) C. Olivier, S. Choua, P. Turek, D. Touchard, S. Rigaut, *Chem. Commun.* **2007**, 3100-3102; l) B. Albinsson, M. P. Eng, K. Pettersson, M. U. Winters, *Phys. Chem. Chem. Phys.* **2007**, *9*, 5847-5864; m) B. Albinsson, J. Mårtensson, *J. Photochem. Photobiol., C* **2008**, *9*, 138-155; n) W. B. Davis, W. A. Svec, M. A. Ratner, M. R. Wasielewski, *Nature* **1998**, *396*, 60-63; o) F. Giacalone, J. L. Segura, N. Martín, D. M. Guldi, *J. Am. Chem. Soc.* **2004**, *126*, 5340-5341; p) R. T. Hayes, M. R. Wasielewski, D. Gosztola, *J. Am. Chem. Soc.* **2000**, *122*, 5563-5567; q) K. E. Linton, M. A. Fox, L.-O. Pålsson, M. R. Bryce, *Chem. Eur. J.* **2015**, *21*, 3997-4007; r) A. B. Ricks, K. E. Brown, M. Wenninger, S. D. Karlen, Y. A. Berlin, D. T. Co, M. R. Wasielewski, *J. Am. Chem. Soc.* **2012**, *134*, 4581-4588; s) A. Arrigo, A. Santoro, F. Puntoriero, P. P. Lainé, S. Campagna, *Coord. Chem. Rev.* **2015**, *304*, 109-116; t) P. Jarosz, K. Lotito, J. Schneider, D. Kumaresan, R. Schmehl, R. Eisenberg, *Inorg. Chem.* **2009**, *48*, 2420-2428; u) C. D. Cruz, P. R. Christensen, E. L. Chronister, D. Casanova, M. O. Wolf, C. J. Bardeen, *J. Am. Chem. Soc.* **2015**, *137*, 12552-12564; v) Y. Luo, K. Barthelmes, M. Wächtler, A. Winter, U. S. Schubert, B. Dietzek, *J. Phys. Chem. C* **2017**, *121*, 9220-9229; w) M. Delor, T. Keane, P. A. Scattergood, I. V. Sazanovich, G. M. Greetham, M. Towrie, A. J. H. M. Meijer, J. A. Weinstein, *Nat Chem* **2015**, *7*, 689-695.

[4] a) J. Melomedov, J. R. Ochsmann, M. Meister, F. Laquai, K. Heinze, *Eur. J. Inorg. Chem.* **2014**, *2014*, 1984-2001; b) A. Magnuson, M. Anderlund, O. Johansson, P. Lindblad, R. Lomoth, T. Polivka, S. Ott, K. Stensjö, S. Styring, V. Sundström, L. Hammarström, *Acc. Chem. Res.* **2009**, *42*, 1899-1909.

[5] a) M. Yamamoto, J. Föhlinger, J. Petersson, L. Hammarström, H. Imahori, *Angew. Chem. Int. Ed.* **2017**, *56*, 3329-3333; b) F. M. Toma, F. Puntoriero, T. V. Pho, M. La Rosa, Y. S. Jun, B. J. T. de Villers, J. Pavlovich, G. D. Stucky, S. Campagna, F. Wudl, *Angew. Chem. Int. Ed.* **2015**, *54*, 6775-6779; c) D. Polyansky, D. Cabelli, J. T. Muckerman, E. Fujita, T. Koizumi, T. Fukushima, T. Wada, K. Tanaka, *Angew. Chem. Int. Ed.* **2007**, *46*, 4169-4172; d) J. H. Klein, T. L. Sunderland, C. Kaufmann, M. Holzapfel, A. Schmiedel, C. Lambert, *Phys. Chem. Chem. Phys.* **2013**, *15*, 16024-16030; e) K. Kitamoto, K. Sakai, *Chem. Eur. J.* **2016**, *22*, 12381-12390.

[6] a) O. Varnavski, P. Bäuerle, T. Goodson III, *Opt. Lett.* **2007**, *32*, 3083-3085; b) C.-K. Yong, P. Parkinson, D. V. Kondratuk, W.-H. Chen, A. Stannard, A. Summerfield, J. K. Sprafke, M. C. O'Sullivan, P. H. Beton, H. L. Anderson, L. M. Herz, *Chem. Sci.* **2015**, *6*, 181-189.

[7] a) J. E. Barnsley, G. E. Shillito, C. B. Larsen, H. van der Salm, L. E. Wang, N. T. Lucas, K. C. Gordon, *J. Phys. Chem. A* **2016**, *120*, 1853-1866; b)

C. B. Larsen, H. van der Salm, C. A. Clark, A. B. S. Elliott, M. G. Fraser, R. Horvath, N. T. Lucas, X.-Z. Sun, M. W. George, K. C. Gordon, *Inorg. Chem.* **2014**, *53*, 1339-1354; c) C. B. Larsen, H. van der Salm, G. E. Shillito, N. T. Lucas, K. C. Gordon, *Inorg. Chem.* **2016**, *55*, 8446-8458; d) K. R. Justin Thomas, J. T. Lin, M. Velusamy, Y. T. Tao, C. H. Chuen, *Adv. Funct. Mater.* **2004**, *14*, 83-90.

[8] a) T. Higashino, T. Yamada, M. Yamamoto, A. Furube, N. V. Tkachenko, T. Miura, Y. Kobori, R. Jono, K. Yamashita, H. Imahori, *Angew. Chem., Int. Ed.* **2016**, *55*, 629-633; b) S.-H. Lee, A. G. Larsen, K. Ohkubo, Z.-L. Cai, J. R. Reimers, S. Fukuzumi, M. J. Crossley, *Chem. Sci.* **2012**, *3*, 257-269; c) M. R. Wasielewski, D. G. Johnson, W. A. Svec, K. M. Kersey, D. W. Minsek, *J. Am. Chem. Soc.* **1988**, *110*, 7219-7221.

[9] a) M. Kuss-Petermann, O. S. Wenger, *J. Am. Chem. Soc.* **2016**, *138*, 1349-1358; b) M. Kuss-Petermann, O. S. Wenger, *Angew. Chem., Int. Ed.* **2016**, *55*, 815-819.

[10] a) L. Troian-Gautier, E. E. Beauvilliers, W. B. Swords, G. J. Meyer, *J. Am. Chem. Soc.* **2016**, *138*, 16815-16826; b) M. Natali, F. Scandola, *J. Phys. Chem. A* **2016**, *120*, 1588-1600.

[11] a) T. Scherer, I. Van Stokkum, A. Brouwer, J. Verhoeven, *J. Phys. Chem.* **1994**, *98*, 10539-10549; b) W. Jäger, S. Schneider, J. Verhoeven, *Chem. Phys. Lett.* **1997**, *270*, 50-58.

[12] a) G. L. Gaines III, M. P. O'Neil, W. A. Svec, M. P. Niemczyk, M. R. Wasielewski, *J. Am. Chem. Soc.* **1991**, *113*, 719-721; b) P. F. Barbara, T. J. Meyer, M. A. Ratner, *J. Phys. Chem.* **1996**, *100*, 13148-13168.

[13] a) S. I. Druzhinin, N. P. Ernsting, S. A. Kovalenko, L. P. Lustres, T. A. Senyushkina, K. A. Zachariasse, *J. Phys. Chem. A* **2006**, *110*, 2955-2969; b) S. I. Druzhinin, V. A. Galievsky, A. Demeter, S. A. Kovalenko, T. Senyushkina, S. R. Dubbaka, P. Knochel, P. Mayer, C. Grosse, D. Stalke, K. A. Zachariasse, *J. Phys. Chem. A* **2015**, *119*, 11820-11836.

[14] a) S. Fukuzumi, K. Ohkubo, Y. Tokuda, T. Suenobu, *J. Am. Chem. Soc.* **2000**, *122*, 4286-4294; b) D. V. Matyushov, *J. Phys. Chem. Lett.* **2012**, *3*, 1644-1648; c) H. B. Kim, N. Kitamura, Y. Kawanishi, S. Tazuke, *J. Am. Chem. Soc.* **1987**, *109*, 2506-2508.

[15] a) A. M. Napper, N. J. Head, A. M. Oliver, M. J. Shephard, M. N. Paddon-Row, I. Read, D. H. Waldeck, *J. Am. Chem. Soc.* **2002**, *124*, 10171-10181; b) A. M. Napper, I. Read, N. J. Head, A. M. Oliver, M. N. Paddon-Row, *J. Am. Chem. Soc.* **2000**, *122*, 5220-5221; c) A. M. Napper, I. Read, R. Kaplan, M. B. Zimmt, D. H. Waldeck, *J. Phys. Chem. A* **2002**, *106*, 5288-5296; d) I. Read, A. Napper, R. Kaplan, M. B. Zimmt, D. H. Waldeck, *J. Am. Chem. Soc.* **1999**, *121*, 10976-10986.

Entry for the Table of Contents

COMMUNICATION

We herein communicate a D-A-A triad that acts as a proof-of-concept for a photoinitiated molecular circuit, whereupon geometric rearrangement in a charge-separated excited state facilitates unidirectional electron-transfer around a complete circuit.

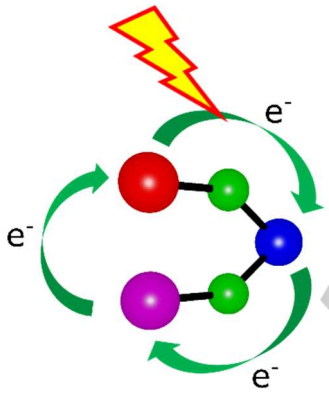

Christopher B. Larsen and Oliver S. Wenger**

Page No. – Page No.

Circular Photoinduced Electron Transfer in a Donor-Acceptor-Acceptor Triad